

## Deuteron-gamma angular correlations in the reactions $^{24,26}\text{Mg}, ^{28,30}\text{Si}(d,d_1\gamma)$ at $E_d = 10 \text{ MeV}$

F. Vogler, J. Böttcher, W. Eyrich, A. Hofmann, M. Meyer, and U. Scheib

*Physikalisches Institut der Universität Erlangen-Nürnberg, D-8520 Erlangen, Federal Republic of Germany*

(Received 7 March 1983)

We measured differential cross sections and  $d_1$ - $\gamma$  angular correlations for the scattering of 10 MeV deuterons on  $^{24}\text{Mg}$ ,  $^{26}\text{Mg}$ ,  $^{28}\text{Si}$ , and  $^{30}\text{Si}$ . The data were analyzed in terms of coupled channels in a  $0^+ \rightarrow 2^+$  coupling scheme on the basis of a symmetric rigid rotator model and in the framework of the distorted wave Born approximation. The correlation data of  $^{24,26}\text{Mg}$  show a remarkable prolate-oblate sensitivity. They can be described also in the distorted wave Born approximation, but only in the prior interaction form. For  $^{30}\text{Si}$  multistep processes can be indicated. The results are consistent with a prolate nuclear shape of  $^{30}\text{Si}$ .

|  |
|--|
| <p style="margin: 0;">NUCLEAR REACTIONS <math>^{24,26}\text{Mg}, ^{28,30}\text{Si}(d,d_1\gamma)</math>, <math>E_d = 10 \text{ MeV}</math>; measured in-plane <math>d_1</math>-<math>\gamma</math> correlations. <math>^{24,26}\text{Mg}, ^{28,30}\text{Si}</math> deduced prolate-oblate nuclear shape, restriction of optical model parameters. Coupled channels and DWBA analyses, enriched targets.</p> |
|--|

### I. INTRODUCTION

By particle  $\gamma$ -angular correlations it is possible to determine the polarization of excited nuclear states. As phases between reaction amplitudes enter into the description of the magnetic substate population, particle  $\gamma$ -angular correlations yield a sensitive tool in nuclear structure and reaction mechanism studies. This has been demonstrated in a series of investigations (see, e.g., Refs. 1–6). For example,  $(\alpha, \alpha'\gamma)$  measurements with  $\alpha$  particles of 104 MeV yielded a unique determination of the sign of the deformation for  $sd$ -shell nuclei.<sup>6</sup> The results could be interpreted not only by coupled channels calculations but also within a simple picture of Fraunhofer diffraction. It was one aim of the present work to see to what extent the results of 104 MeV  $\alpha$  scattering could be transformed to the scattering of 10 MeV deuterons, where, due to the large number of open channels, compound nucleus contributions are expected to be small. On the other hand, we emphasized in a previous work<sup>7</sup> that the analysis of angular correlation data can be a powerful way of determining nuclear reaction mechanisms. This was demonstrated by comparing differential cross sections and in-plane  $(d, d_1\gamma)$  angular correlations of the inelastic deuteron scattering on  $^{24}\text{Mg}$  at  $E_d = 10 \text{ MeV}$  with coupled channels (CC) and distorted wave Born approximation (DWBA) calculations, respectively. Only the CC calculations were found to be able to reproduce the angular correlation data whereas the cross sections can be described with CC and DWBA calculations as well. From this we concluded that multistep processes are important for this reaction and that the DWBA cannot be assumed to be an adequate reaction model solely from the fact that it can describe differential cross sections.

In the meantime we have continued these investigations. We found that there are DWBA calculations which indeed lead to a reasonable description also of the angular correlation data. It seems to be most remarkable, however, that the only DWBA calculations which succeed in describing the  $^{24}\text{Mg}(d, d_1\gamma)$  data are those in which the prior interac-

tion form is used. (The DWBA calculations in Ref. 7 have been performed exclusively with the post interaction form.) From these results, it is suggested that the conditions under which the DWBA will be able to simulate CC effects should be investigated. Recently this question was also discussed by Ascuitto *et al.*<sup>8</sup> They analyzed the  $^{16}\text{O} + ^{40}\text{Ca}$  system, finding the DWBA to be an adequate model for the description of inelastic cross sections, if the exit-channel distorting potential is chosen correctly. A procedure for choosing it is discussed. In this context it seemed worthwhile to extend our investigations to some other nuclei. We measured again in-plane  $(d, d_1\gamma)$  angular correlations together with differential cross sections at  $E_d = 10 \text{ MeV}$  on  $^{26}\text{Mg}$ ,  $^{28}\text{Si}$ , and  $^{30}\text{Si}$ . The individual properties of these neighboring even-even nuclei are of special interest for our studies. Considering the sign and magnitude of deformation,  $^{26}\text{Mg}$  can be assumed to behave similarly to  $^{24}\text{Mg}$ , whereas  $^{28}\text{Si}$  is known to be negatively deformed. Among these four nuclei,  $^{30}\text{Si}$  is the only case in which the differential cross section of the inelastic scattering to the first excited state can be described by a "symmetric" DWBA (i.e., one in which the elastic scattering optical potential is used also as the exit-channel distorting potential).

### II. EXPERIMENT

We measured for the nuclei  $^{26}\text{Mg}$ ,  $^{28}\text{Si}$ , and  $^{30}\text{Si}$  differential cross sections for elastic and inelastic deuteron scattering and  $d_1$ - $\gamma$  double differential cross sections of in-plane angular correlations at the Erlangen EN tandem accelerator at a bombarding energy of 10 MeV.<sup>9</sup> As targets we used self-supporting foils, apart from  $^{30}\text{Si}$  where we used  $^{30}\text{SiO}_2$ , with areal densities of  $(1.2 \pm 0.05) \times 10^{19} / \text{cm}^2$  for  $^{26}\text{Mg}$ ,  $(13 \pm 0.3) \times 10^{19} / \text{cm}^2$  for  $^{28}\text{Si}$  and  $(1.8 \pm 0.05) \times 10^{19} / \text{cm}^2$  for  $^{30}\text{Si}$ . The differential cross sections were measured in a conventional way by use of  $\Delta E$ - $E$  surface barrier detector telescopes. In the angular correlation experiments surface barrier detectors, placed at fixed angles between  $30^\circ$  and  $100^\circ$ , were used for

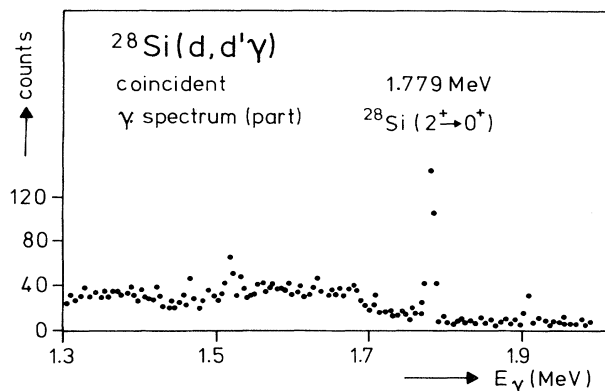


FIG. 1.  $\gamma$  spectrum coincident with deuterons scattered at an angle of  $65^\circ$  from the reaction  $^{28}\text{Si}(d,d'\gamma)$  for the  $\gamma$  detector at  $-65^\circ$ . The  $\gamma$  energy resolution is about 9 keV.

the detection of the scattered deuterons. Up to eight particle detectors were mounted in a distance of 10 to 11.5 cm to the target. Rectangular slits with solid angles from 1.6 msr up to 3.6 msr were used. The energy resolution for the scattered deuterons was about 60 to 100 keV according to the kinematics. The  $\gamma$  radiation was measured by two Ge(Li) detectors having efficiencies of 10% and 8% in comparison with a 7.6 cm  $\times$  7.6 cm NaI detector, respectively. Lead collimators defined the solid angle of the Ge(Li) detectors, in front of which a thin layer of lead shielded against a low energy background. The opening angle was  $\pm 7^\circ$  or  $\pm 9^\circ$ , respectively, so that the correction of the angular correlation function due to the finite angle was negligible. Especially in the case of the  $^{30}\text{SiO}_2$  target the use of a Ge(Li)  $\gamma$  detector was essential due to the complexity of the  $\gamma$  spectra. The total  $\gamma$ -energy resolution in the experiment was  $\sim 9$  keV. Each of the  $\gamma$  detectors worked in coincidence with all particle detectors. In this way  $d_1$ - $\gamma$  coincidence spectra were measured for five positions of the  $\gamma$  detectors. In order to give an impression of our data, in Fig. 1 a  $\gamma$  spectrum coincident with deuterons scattered at a particular angle is shown for the reaction  $^{28}\text{Si}(d,d'\gamma)$  as an example. In the coincident  $\gamma$  spectra also for the other nuclei, the corresponding  $2^+ \rightarrow 0^+$  transition appears nearly free of background so that the extraction of the double differential cross sections from the photopeak area was possible without any problems. More details about the experimental setup and the data evaluation are described in Ref. 10. To present the results of our angular correlation measurements and their analysis we use the in-plane angular correlation function which is obtained from the measured double differential cross section. The double differential cross section follows from the number of coincident counts in the photopeak of interest  $N_{\text{coin}}$ , the areal density  $N_F$  of the target, the number of incoming deuterons  $j$ , the particle detector solid angle  $d\Omega_d$ , the  $\gamma$ -detector solid angle  $d\Omega_\gamma$ , and the  $\gamma$ -detector photopeak efficiency  $\epsilon_\gamma$

$$\frac{d^2\sigma}{d\Omega_d d\Omega_\gamma} = \frac{N_{\text{coin}}}{N_F j d\Omega_d \epsilon_\gamma d\Omega_\gamma}.$$

The error for the double differential cross section was on

the order of  $\sim 10\%$  for  $N_{\text{coin}}$  (statistical error) and about 7% for the rest, which together with the error in the differential cross section led to an error for the angular correlation function of  $\leq 15\%$ . In order to check the reproducibility of the data, we measured overlapping angular settings, which generally led to fair agreement within these error bars. In the case of deuteron scattering to a  $2^+$  state of an even-even nucleus with subsequent  $\gamma$  deexcitation to a  $0^+$  state one has

$$W(\phi_\gamma) = 4\pi \frac{d^2\sigma}{d\Omega_d d\Omega_\gamma} \bigg/ \frac{d\sigma}{d\Omega_d} \\ = A + B \sin^2(\phi_\gamma - \phi_1) + C \sin^2 2(\phi_\gamma - \phi_2).$$

$\phi_\gamma$  is the angle between the beam direction and the  $\gamma$  detector. The parameters  $A$ ,  $B$ ,  $C$ ,  $\phi_1$ , and  $\phi_2$  depend on the deuteron scattering angle and are functions of the reaction amplitudes for transitions between the magnetic substates of the entrance and exit channels.<sup>11</sup> Since the parameters of the angular correlation function contain combinations of the reaction amplitudes other than the differential cross section, which is proportional to the sum of the absolute squares of all reaction amplitudes, the angular correlation function is able to yield additional information about nuclear structure and reaction mechanism.

The values for the parameters  $A$ ,  $C$ , and  $\phi_2$  were determined by fitting our angular correlation data with an angular correlation function according to Eq. (1) neglecting the so-called spin-flip term  $B$ , which is important only at very backward angles. The  $\chi^2$  values of the fits of Eq. (1) to our experimental data, neglecting the parameter  $B$ , were within the confidence limit. Therefore, we assumed  $B = 0$ , i.e., we neglected "spin-flip" processes in our analyses. The values of  $B$  calculated within the DWBA and the CC formalism, respectively, also prove to be very small in the angular region considered.

### III. RESULTS AND DISCUSSION

For the present analysis of our data we have used the DWBA code DWUCK (Ref. 13) and the coupled channels code ECIS (Ref. 14) modified for the calculation of the angular correlation.<sup>15</sup> First we tried to find an optimum description of the differential cross section. With the parameters so obtained we calculated angular correlations. We concentrated mostly on the discussion of the angular correlation parameter  $C$ , which turned out to be very useful in the  $(\alpha, \alpha'\gamma)$  correlations at  $E_\alpha = 104$  MeV.<sup>6</sup> At this energy the isotropic part  $A$  of the angular correlation function proved always to be zero, and the phase  $\phi_2$  yielded values close to the adiabatic limit, thus giving no further information. At lower energies  $A$  is strongly influenced by compound nuclear contributions, which, however, should be negligible in the case of d scattering due to the large number of open channels. This has been verified by model calculations of the reaction  $^{28}\text{Si}(d,d'\gamma)$  in which coupled channels and compound contributions were taken into account.<sup>16</sup> Also the phase  $\phi_2$  shows deviations from the adiabatic limit at lower energies, especially in the angular region of cross section minima. The dependence of  $\phi_2$  on the used reaction models, however, is not as pronounced as for the correlation amplitude  $C$ , which we will discuss in the following.

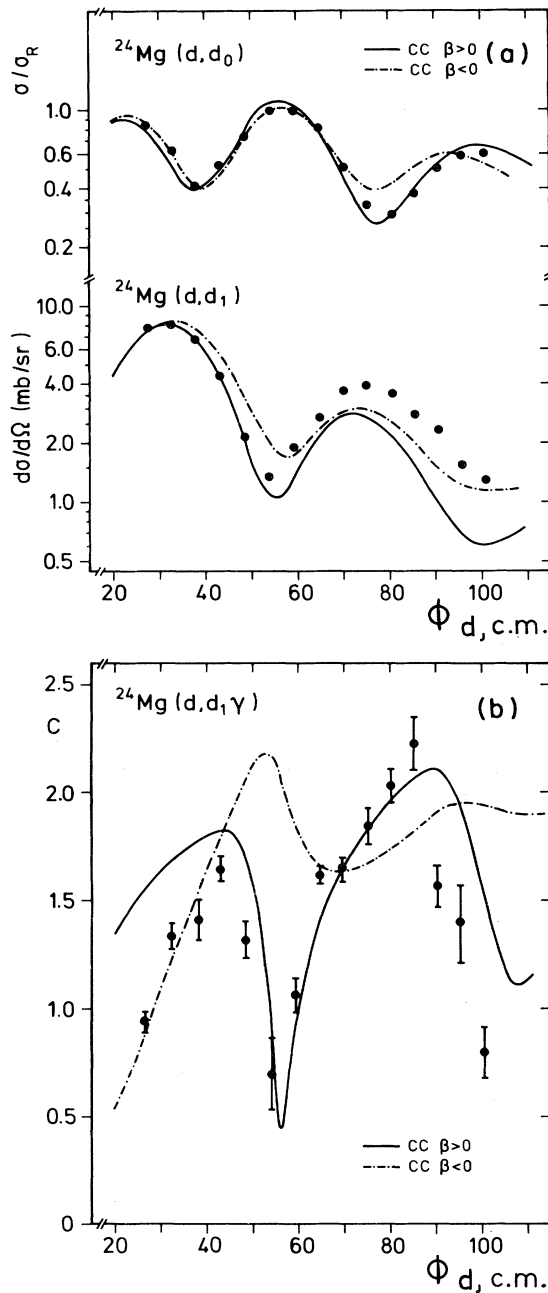


FIG. 2. (a) Differential cross section for the elastic (upper curve) and inelastic (lower curve) scattering to the first  $2^+$  state of 10 MeV deuterons by  $^{24}\text{Mg}$  compared with coupled channels calculations for different signs of the quadrupole deformation  $\beta_2$ . (Optical model parameters are listed in Table I.) (b) Correlation amplitude  $C$  of the in-plane particle  $\gamma$ -correlation data of the reaction  $^{24}\text{Mg}(d,d_1\gamma)$  compared with CC calculations. The calculations correspond to those of the cross sections. The shown error bars contain mainly statistical errors (see Sec. II).

#### A. Coupled channels analyses

The coupled channels calculations have been performed in a  $0^+-2^+$  coupling scheme for a rigid symmetric rotator, mostly for spinless particles. The deuteron spin which did

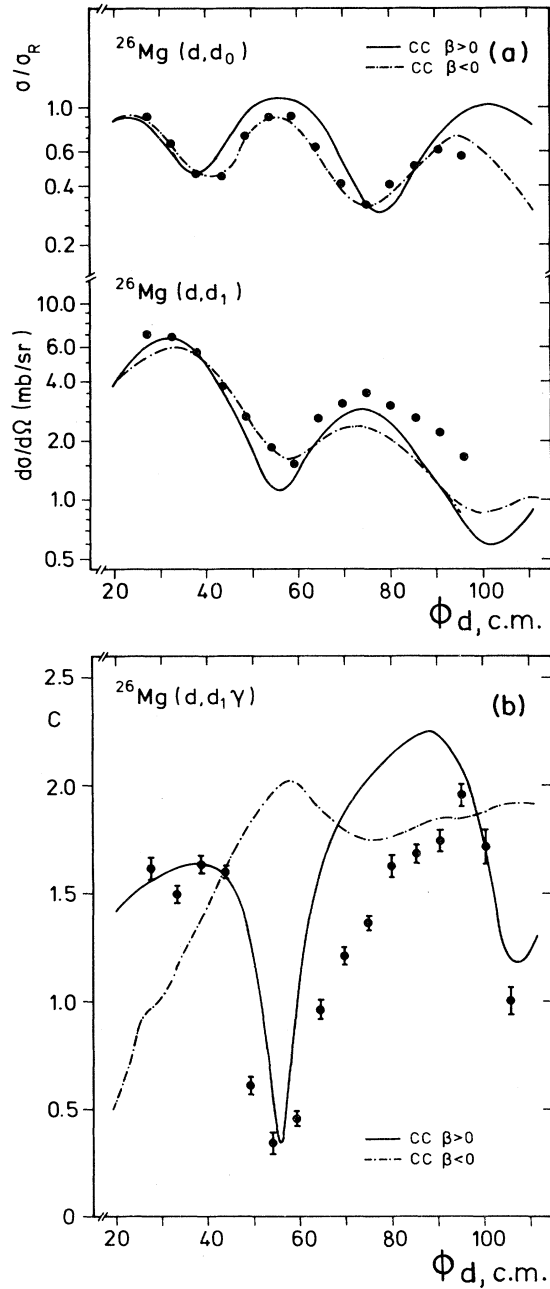


FIG. 3. Same as in Fig. 2 for  $^{26}\text{Mg}$ .

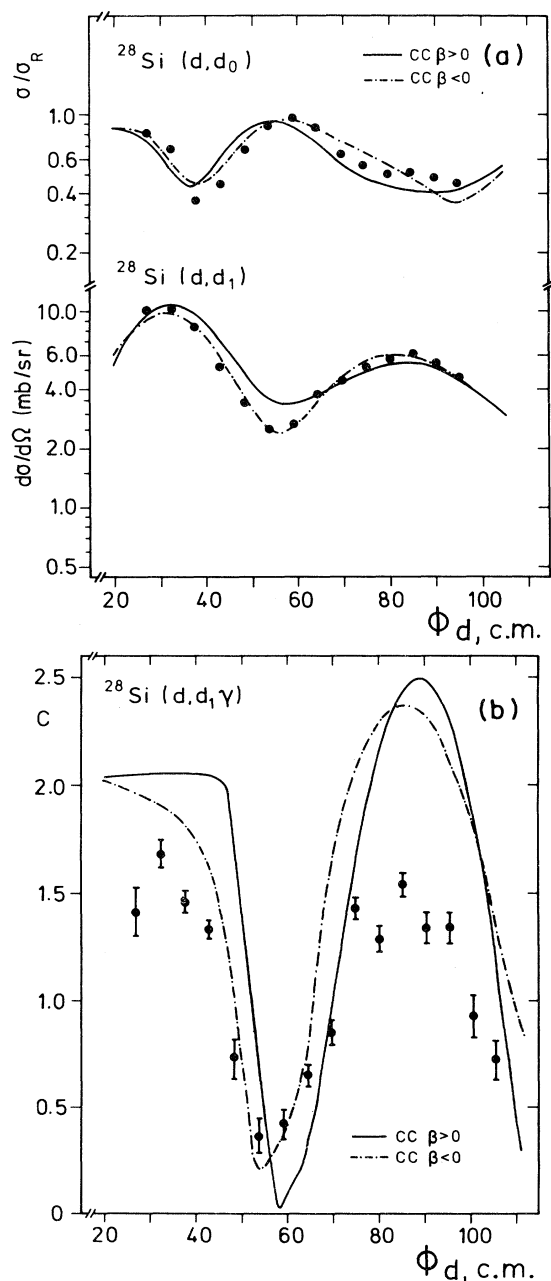
not manifest itself in a  $B$  term in the angular correlation function was found to also have no remarkable influence on other parameters. Especially there is no dependence of  $C$  on the spin-orbit part of the optical potential.<sup>17</sup> It was our objective to see to what extent  $d'$ - $\gamma$  correlations are sensitive to prolate-oblate effects obtained in CC calculations as well as to test the sensitivity of various potential parameters in  $d$  scattering.

#### 1. Prolate-oblate nuclear shape

In Ref. 6 we have shown for  $(\alpha,\alpha'\gamma)$  angular correlations at 104 MeV that a remarkable prolate-oblate sensi-

TABLE I. Parameter sets used in the CC calculations.

|                  | $V$   | $r_V$ | $a_V$ | $W_D$ | $r_W$ | $a_W$ | $V_{SO}$ | $r_{SO}$ | $a_{SO}$ | $\beta_2$ | $\frac{4W_D r_W a_W}{V r_V^2 A^{1/3}}$ | Minimum<br>in $C$ |
|------------------|-------|-------|-------|-------|-------|-------|----------|----------|----------|-----------|--|-------------------|
| $^{24}\text{Mg}$ | 105.0 | 1.54  | 0.50  | 16.0  | 1.13  | 0.83  | 6.0      | 1.54     | 0.50     | + 0.42    | 0.083                                  | yes               |
| $^{24}\text{Mg}$ | 105.0 | 1.63  | 0.47  | 39.8  | 1.13  | 0.59  |          |          |          | -0.51     | 0.132                                  | no                |
| $^{26}\text{Mg}$ | 105.0 | 1.54  | 0.43  | 18.0  | 1.04  | 0.80  |          |          |          | + 0.40    | 0.081                                  | yes               |
| $^{26}\text{Mg}$ | 100.0 | 1.31  | 0.63  | 26.0  | 1.34  | 0.61  |          |          |          | -0.53     | 0.169                                  | no                |
| $^{28}\text{Si}$ | 137.2 | 1.14  | 0.65  | 7.04  | 1.90  | 0.57  |          |          |          | + 0.31    | 0.057                                  | yes               |
| $^{28}\text{Si}$ | 115.7 | 1.04  | 0.59  | 7.06  | 1.85  | 0.56  |          |          |          | -0.38     | 0.076                                  | yes               |
| $^{30}\text{Si}$ | 70.45 | 1.42  | 0.69  | 18.48 | 1.63  | 0.39  | 3.8      | 1.2      | 0.7      | + 0.21    | 0.106                                  | yes               |
| $^{30}\text{Si}$ | 90.69 | 1.19  | 0.74  | 10.54 | 1.58  | 0.59  | 6.81     | 1.2      | 0.7      | -0.26     | 0.100                                  | yes               |

FIG. 4. Same as in Fig. 2 for  $^{28}\text{Si}$ .

tivity of the angular correlation amplitude  $C$  exists not only in the coupled channels calculation but nearly model independently as can be shown with the aid of Fraunhofer diffraction scattering.

In order to see whether this holds also for 10 MeV deuterons we considered first  $^{24}\text{Mg}$  as a well-known case of positive (prolate) deformation. The upper part of Fig. 2 shows the differential cross sections for elastic and inelastic (leading to the first  $2^+$  state) scattering of 10 MeV deuterons on  $^{24}\text{Mg}$ . The curves correspond to best-fit calculations for positive and negative quadrupole deformation ( $\beta$ ), respectively. The parameters used in these calculations (and in the calculations for  $^{26}\text{Mg}$ ,  $^{28}\text{Si}$ , and  $^{30}\text{Si}$  as discussed later) are shown in Table I. Whereas the cross section data would not allow a determination of the sign of  $\beta$ , the angular dependence of the correlation quantity  $C$  clearly can only be reproduced by the calculation for  $\beta > 0$  as can be seen from the lower part of Fig. 2. The pronounced minimum at  $\phi_d \approx 55^\circ$  seems especially to be a characteristic feature of the deformation sign.

For  $^{26}\text{Mg}$  the deformation character was not as unambiguously determined as in the case of  $^{24}\text{Mg}$  from analyses of scattering data<sup>18</sup> though measurements of the Coulomb reorientation effect<sup>19</sup> and an  $(\alpha, \alpha'\gamma)$  experiment<sup>20</sup> at  $E_\alpha = 104$  MeV yielded a positive value for the  $\beta$  deformation. In Fig. 3 the results for deuteron scattering at 10 MeV are displayed. The angular correlation shows behavior similar to that in the case of  $^{24}\text{Mg}$ . The minimum in the angular dependence of  $C$  is not obtained by the calculation for oblate shape.

It is known—for example, from  $(\alpha, \alpha'\gamma)$  angular correlations<sup>21</sup>—that  $^{28}\text{Si}$  is an oblate shaped nucleus. This statement cannot be made from the  $(d, d')$  reaction. In Fig. 4 the differential cross section and the angular correlation data are compared with calculations for positive and negative deformation. Even the angular correlation allows no discrimination between both calculations for different signs of  $\beta$ . In spite of the negative deformation, the experimental data exhibit a clear minimum at  $\phi_d \approx 55^\circ$  which can be reproduced by both calculations. As we shall discuss later, the appearance of this minimum is due to the ratio of the absorptive part to the real part of the used optical potential. Therefore it cannot be used in general to decide about the sign of the nuclear deformation.

Certainly the most interesting nucleus from the theoretical point of view is  $^{30}\text{Si}$ , for which a determination of the quadrupole deformation seemed highly desirable. Several Hartree-Fock-Bogoliubov calculations<sup>22</sup> suggest negative  $\beta$  deformation whereas truncated shell model calculations<sup>23</sup>

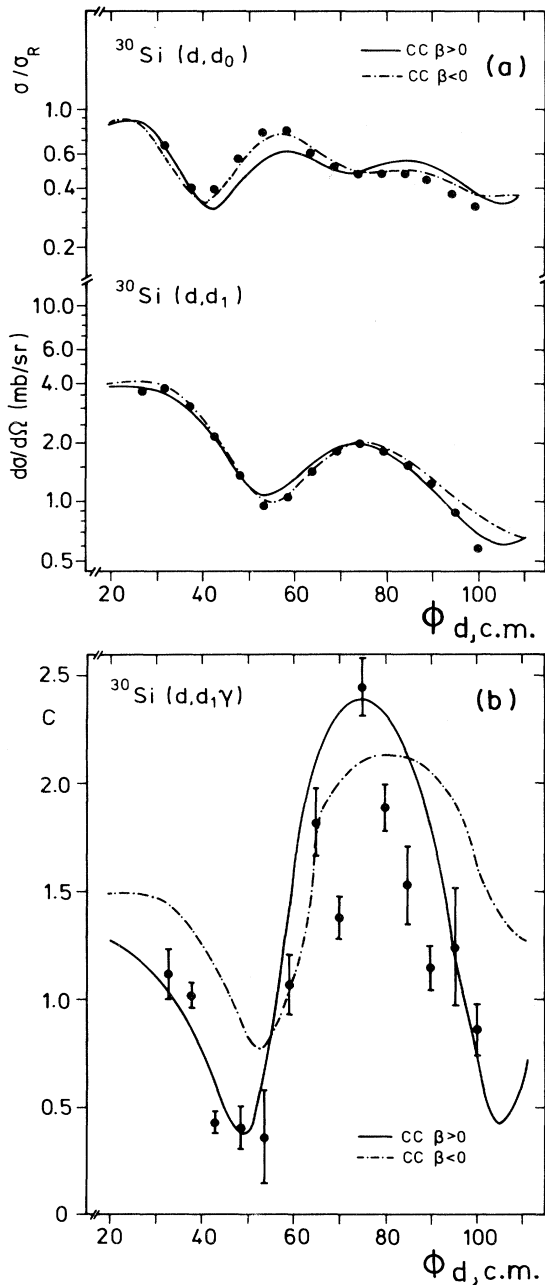


FIG. 5. Same as in Fig. 2 for  $^{30}\text{Si}$ .

predicted positive  $\beta$  values. An earlier analysis of d-scattering data yielded positive quadrupole deformation.<sup>24</sup> Besides that, we know of only one Coulomb reorientation measurement<sup>25</sup> which yields a small negative quadrupole moment, i.e., positive quadrupole deformation. The opposite sign is excluded by the authors, assuming constructive interference from the second excited state. Figure 5 shows our angular distribution of the differential cross sections for elastic and inelastic ( $2^+$ ) deuteron scattering and again the correlation amplitude  $C$  along with coupled channel calculations for positive and negative  $\beta$  values, respectively.

The angular correlation data agree very well with the

CC calculation for a positive  $\beta_2$  deformation and are consistent with a prolate shape of  $^{30}\text{Si}$ . The strength of deformation ( $\beta = +0.21$ ) which is already fixed by the fits of the differential cross section agrees rather well with the value favored by the  $^{30}\text{Si}$  reorientation experiment.<sup>25</sup>

## 2. Restriction of parameters within a collective model

In basing the description of the scattering from a nucleus on a certain microscopic model, one often has difficulties in the restriction of the used potential parameters. In the following section we explore—using the rotational model in conjunction with  $0^+-2^+$  coupling—to what extent the  $d'-\gamma$  angular correlation is sensitive to potential parameters, especially the absorption potential. Often a more detailed knowledge of the strength of the absorption potential than is available from cross section analyses is desirable. Especially in the context of folding model analyses it is the only quantity which is not fixed by empirical data. Glanz and Rawitscher<sup>26</sup> have indeed shown, in a theoretical example, that substate populations which could be determined from  $(\alpha, \alpha'\gamma)$  correlations would differ considerably for different strengths of the absorption potential. Clement *et al.*<sup>27</sup> have shown that in CC analyses of cross sections and vector analyzing powers of deuterons one could start from standard potentials after Lohr and Haeblerli,<sup>28</sup> whereby only the magnitude of  $\beta$  and the absorption potential has to be changed. The study of the amplitude  $C$  of the  $d'-\gamma$  angular correlation has the obvious advantage of only a small dependence on the magnitude of  $\beta$ , since only the ratio of reaction amplitudes enters into  $C$ .<sup>6</sup> We therefore concentrate our discussion on the absorption, which is well described for 10 MeV deuterons with a surface term.

In the previous section we saw that coupled channel calculations assuming (the wrong) oblate deformation for  $^{24}\text{Mg}$  and  $^{26}\text{Mg}$  lead to no minimum in the correlation amplitude  $C$  of the  $(d, d'\gamma)$  correlation (cf. Figs. 2 and 3). Since in both cases a big strength of the absorption potential  $W$  was necessary in order to describe the cross sections, we had an indication of a connection between the nonexistence of the minimum in  $C$  and the potential strength  $W_D$ . This was confirmed by the occurrence of a minimum of  $C$  in the  $(d, d'\gamma)$  reaction on  $^{28}\text{Si}$  and  $^{30}\text{Si}$  which was obtained by prolate as well as oblate deformation. In both cases the potential depth  $W_D$  was rather small.

It turned out that for all of our  $0^+-2^+$  calculations the occurrence of a minimum in  $C$  is correlated with the ratio of imaginary and real parts of the interaction potential. Obviously, not the depth but the interaction volume of the potential is important. A measure for these volumes is given by  $Vr^2A^{2/3}$  for the real part and by  $WawrWA^{1/3}$  for the surface imaginary part. In the last column of Table I we quote the ratios of these interaction volumes. One can see that a minimum in  $C$  occurs in all cases where this ratio does not exceed a certain value ( $\leq 0.11$ ).

## B. DWBA analyses

The DWBA has proven to be very successful in the description of many nuclear reactions. In a previous work,<sup>29</sup> DWBA fits for inelastic deuteron scattering on a

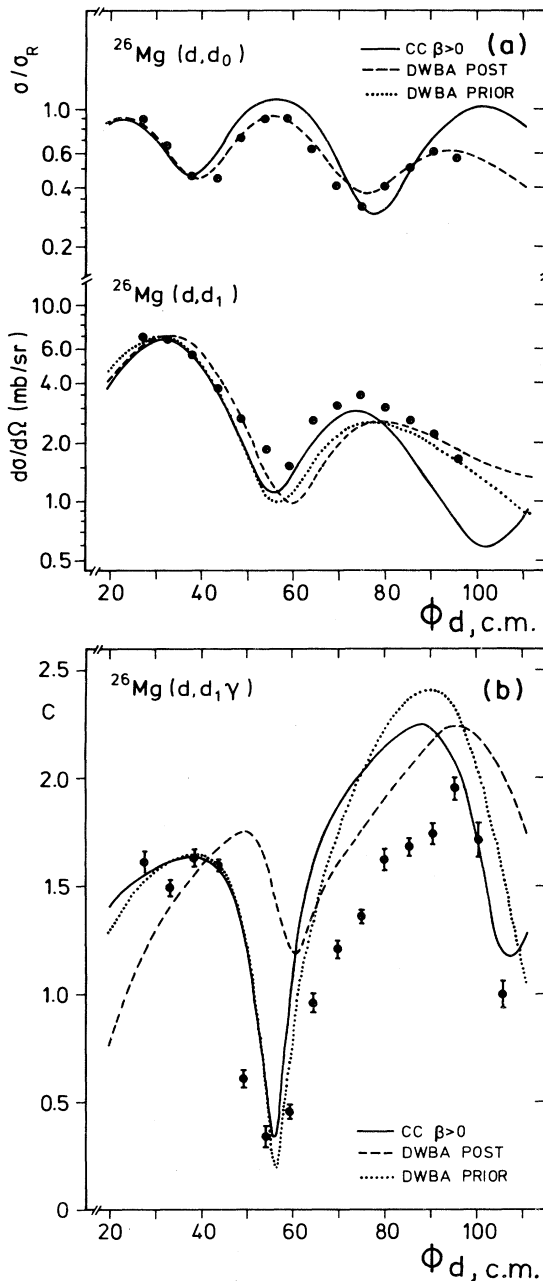


FIG. 6. (a) Differential cross section for the elastic (upper curve) and inelastic (lower curve) scattering to the first  $2^+$  state of 10 MeV deuterons by  $^{26}\text{Mg}$  compared with the coupled channels calculation for prolate deformation and DWBA calculation in post interaction and prior interaction form. (Optical model parameters are listed in Table II.) (b) Correlation amplitude  $C$  of the in-plane particle  $\gamma$ -correlation data of the reaction  $^{26}\text{Mg}(d,d_1\gamma)$  compared with CC and DWBA calculations. The calculations correspond to those of the cross sections. The error bars shown contain mainly statistical errors (see Sec. II).

series of  $sd$  shell nuclei have been made. It turned out that only the  $^{30}\text{Si}$  cross section data could be described with parameter sets being the same for entrance and exist channels, whereas asymmetric sets were needed for  $^{24}\text{Mg}$ ,

$^{26}\text{Mg}$ , and  $^{28}\text{Si}$ . The question arises whether these asymmetries in the DWBA are due to underlying CC effects. Since these nuclei are strongly deformed we would expect that channel coupling plays an important role. It has been shown indeed, in a previous study,<sup>7</sup> that for deuteron scattering on  $^{24}\text{Mg}$  the differential cross sections can be reproduced by the DWBA whereas the amplitude  $C$  of the  $(d,d_1\gamma)$  angular correlation is only described by CC calculations. From this behavior it has been concluded that the minimum in  $C$  is connected with the existence of multistep processes as they are taken into account in the coupled channel formalism. In that case an asymmetric DWBA was used for the description; i.e., the potentials for the calculation of the distorted waves were different in entrance and exit channels, respectively. The form factor was calculated by use of the potential parameters of the exit channel (so-called "post interaction form"). Now, surprisingly, the analysis of the  $^{26}\text{Mg}$  data has shown that one is able to reproduce the minimum in  $C$  even by DWBA, but only if one uses the potential parameters of the entrance channel ("prior interaction form") instead of those of the exit channel for the calculation of the form factor. Figure 6 shows the DWBA calculations for post interaction and prior interaction forms and again the CC calculation of Fig. 3 for  $\beta > 0$  compared with the elastic and inelastic experimental cross section data. In order to avoid confusion with different arbitrary potential parameter sets, the DWBA calculations were performed with the same parameters for the post interaction and prior interaction forms. They are shown in Table II together with the corresponding parameters for  $^{24}\text{Mg}$ ,  $^{28}\text{Si}$ , and  $^{30}\text{Si}$ . The parameter sets of the entrance channel are optical model best fit parameters to the elastic scattering data. The parameters of the exit channel were chosen so as to describe the inelastic scattering data in the post interaction and prior interaction forms reasonably well. Of course, the parameters thus obtained are not necessarily equivalent to the best fit parameters for the respective form of the DWBA. Detailed investigations, however, showed that calculations with best fit parameters do not impair the statements, which we will make below.

The lower part of Fig. 6 shows the different DWBA calculations and the CC calculation for  $\beta > 0$  of Fig. 2 compared with the experimental values for the correlation amplitude  $C$ . Only the CC calculation and the DWBA calculation in the prior interaction form are able to reproduce the minimum in  $C$ . As mentioned above, the DWBA calculations are not really best fit calculations. By adjusting the parameters in the exit channel, description of all experimental data as good as that by the CC calculation could be achieved in the prior interaction form, whereas in the post interaction form no parameter set could be found giving a reasonable description of the cross section and the correlation amplitude  $C$ , simultaneously. Owing to this behavior of  $^{26}\text{Mg}$  we reanalyzed our  $^{24}\text{Mg}$  data with DWBA. It turned out that, as for  $^{26}\text{Mg}$ , besides the CC calculation with  $\beta > 0$ , the DWBA in the prior interaction form is also able to describe the pronounced minimum in  $C$ .

While we could not find any parameter set for  $^{24}\text{Mg}$  and  $^{26}\text{Mg}$  in the post interaction form which is able to describe all experimental data, in the case of  $^{28}\text{Si}$  both the post interaction and prior interaction forms of the DWBA lead

TABLE II. Parameter sets used in the DWBA calculations.

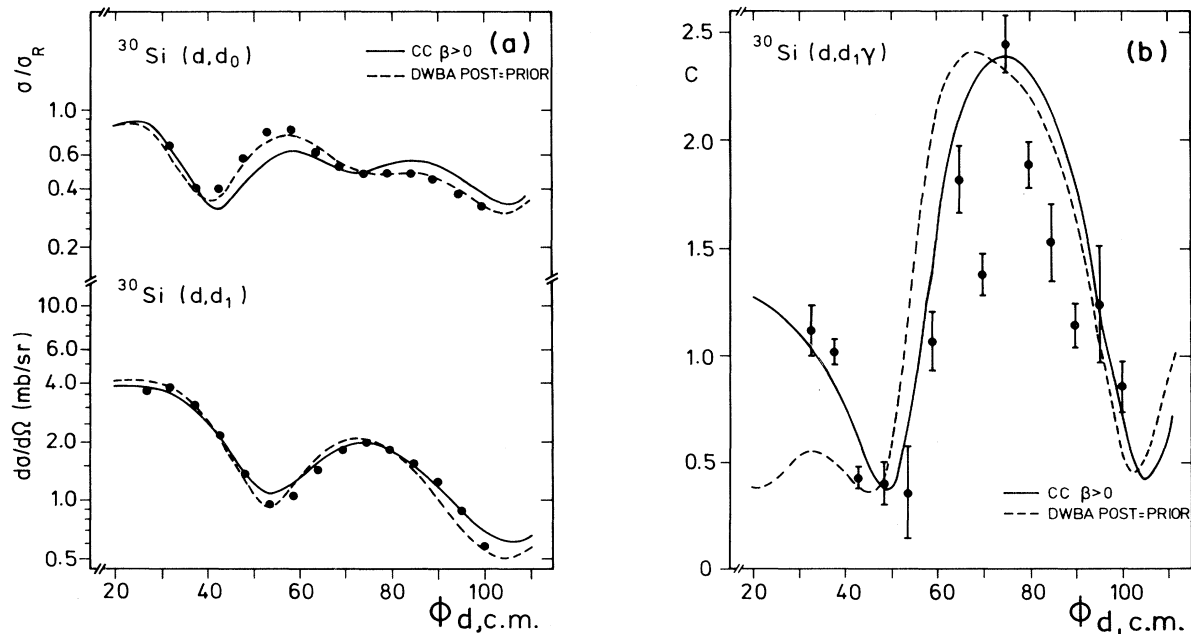
|                  | $V$                  | $r_V$ | $a_V$ | $W_D$ | $r_W$ | $a_W$ | $V_{SO}$ | $r_{SO}$ | $a_{SO}$ | $\beta_2$ |                         |
|------------------|----------------------|-------|-------|-------|-------|-------|----------|----------|----------|-----------|-------------------------|
| $^{24}\text{Mg}$ | Entrance             | 114.8 | 1.32  | 0.53  | 18.5  | 1.06  | 0.89     | 5.5      | 0.98     | 0.98      | Post interaction: 0.44  |
|                  | Exit                 | 109.4 | 1.09  | 0.76  | 17.0  | 1.59  | 0.51     | 5.5      | 0.98     | 0.98      | Prior interaction: 0.59 |
| $^{26}\text{Mg}$ | Entrance             | 114.8 | 1.25  | 0.61  | 27.5  | 1.15  | 0.78     | 5.5      | 0.98     | 0.98      | Post interaction: 0.42  |
|                  | Exit                 | 109.4 | 0.99  | 0.87  | 17.0  | 1.59  | 0.51     | 5.5      | 0.98     | 0.98      | Prior interaction: 0.48 |
| $^{28}\text{Si}$ | Entrance             | 103.1 | 1.14  | 0.80  | 22.3  | 1.56  | 0.49     |          |          |           | Post interaction: 0.68  |
|                  | Exit                 | 100.0 | 1.05  | 0.75  | 15.0  | 1.46  | 0.55     |          |          |           | Prior interaction: 0.38 |
| $^{30}\text{Si}$ | Entrance }<br>Exit } | 97.65 | 1.16  | 0.74  | 17.1  | 1.44  | 0.62     | 6.9      | 0.95     | 0.54      | 0.34                    |

to a reasonable description of differential cross section and angular correlation data. It seems remarkable that the calculations for  $^{24}\text{Mg}$  and  $^{26}\text{Mg}$  need unrealistically large  $\beta$  values for the prior interaction form, whereas in the case of  $^{28}\text{Si}$  one needs a large value of  $\beta$  in the post interaction form (cf. Table II). From the different results for the prior interaction and post interaction forms for  $^{24}\text{Mg}$  and  $^{26}\text{Mg}$ , we do not derive different abilities of both forms to simulate CC effects. In principle, both interaction forms must be equivalent.<sup>30</sup> Nevertheless, their different behavior in the calculation of correlation data should be noticed.

The nucleus  $^{30}\text{Si}$  plays a special role in our discussion because it is the only case where the cross section is reproduced by a symmetric DWBA, i.e., the potential parameters of entrance and exit channels are the same. In Fig. 7 one can see that the differential cross section data for elastic and inelastic scattering is described by DWBA and CC

calculations (for the CC case the prolate solution of Fig. 5 is shown, which is able to fit all data). For the  $(d,d_1\gamma)$  angular correlation only the CC predictions describe the data, whereas (symmetric) DWBA calculations fail to, especially in the forward angle region. It is therefore obvious from the correlation data that for the description of the  $^{30}\text{Si}(d,d')$  reaction inelastic (multistep) processes are essential, which are taken into account in CC calculations.

The extent to which the influence of coupled channels can be simulated by DWBA has been discussed recently by Ascuitto *et al.*<sup>8</sup> in the case of inelastic scattering of  $^{16}\text{O}$  of 60 MeV on  $^{40}\text{Ca}$  leading to various states with spin-parity of  $2^+$ ,  $3^-$ , and  $5^-$ . Rehm *et al.*<sup>31</sup> stated for these transitions that DWBA cannot reproduce the cross sections, whereas CC leads to a significantly better description. This is also true for the  $5^-$  state, although this state is only weakly coupled to the other states. Ascuitto *et al.*<sup>8</sup> show that it is necessary to calculate the distorted waves

FIG. 7. Same as in Fig. 6 for  $^{30}\text{Si}$ .

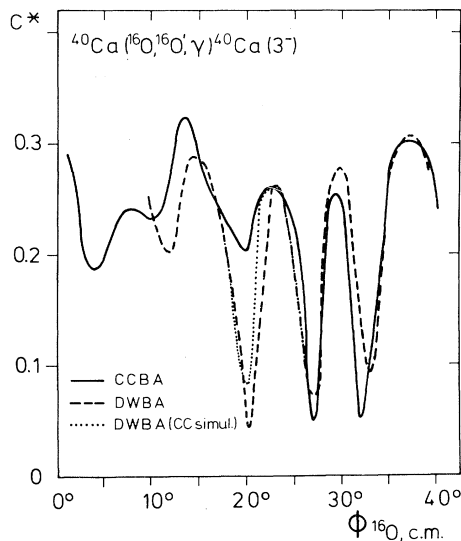


FIG. 8. CC and DWBA calculations for the correlation amplitude  $C^*$  of the in-plane angular correlation of the reaction  $^{40}\text{Ca}(^{16}\text{O}, ^{16}\text{O}'\gamma)^{40}\text{Ca}(3^-)$ , with  $C^* = 5 |X_{M_B} = -3| |X_{M_B} = -3| (d\sigma/d\Omega)^{-1}$  where  $X_{M_B}$  are the reaction amplitudes in the notation of Ref. 11.

with different potentials. With the help of CC calculations they generated so-called “bare-optical potentials” and used these potentials in a DWBA which was asymmetric in referring to entrance and exit channels. In this way they obtained a good description of the cross sections. We tried to extend their simulation method also for the case of stronger coupling like that in the  $^{26}\text{Mg}(d, d')$  reaction, where we have both cross sections and angular correlation data. For that purpose we took best fit values, i.e., for the entrance channel DWBA, for the form factor  $0^+ - 2^+$ , and for the exit channel  $0^+ - 2^+ - 4^+$  CC parameters. This procedure, however, failed even in the description of the cross section. Therefore, we calculated for the case of the  $^{40}\text{Ca}(^{16}\text{O}, ^{16}\text{O}')$  reaction discussed by Ascuitto *et al.*<sup>8</sup> differential cross sections in the framework of CC, DWBA, and an asymmetric DWBA simulating CC ef-

fects, using the procedure suggested in Ref. 8. We were able to reproduce their calculation. It turned out, however, that their DWBA calculations simulating CC effects are equivalent to CC calculations only if one restricts oneself to the cross section. In Fig. 8 the calculations for the amplitude of the  $(^{16}\text{O}, ^{16}\text{O}'\gamma)_{3 \rightarrow 0^+}$  angular correlation function is shown. There are remarkable differences between the CC calculation and the DWBA calculations, even for the one which seems to simulate coupled channels effects, if only the cross section is considered. Therefore, one should not conclude that one is able to simulate CC effects with the aid of DWBA from cross section data.

#### IV. CONCLUDING REMARKS

In conclusion, our coupled channel analyses have shown that remarkable differences for prolate and oblate nuclear shapes are present also in the  $(d, d'\gamma)$  angular correlation of 10 MeV deuterons. However, the big differences in the minimum of the angular correlation amplitudes  $C$  for  $^{24}\text{Mg}$  and  $^{26}\text{Mg}$  are mainly caused by the large values of the absorption potential needed for the description of the cross section data with the (wrong) oblate shape. In the case of  $^{30}\text{Si}$  the angular correlation data are consistent with a prolate nuclear shape in accordance with shell model calculations. From the DWBA analyses it turns out that, in contrast to previous studies, the angular correlation for  $^{24}\text{Mg}$  and  $^{26}\text{Mg}$  can be described also by DWBA. This was only possible, however, for the so-called prior interaction form. The  $^{28}\text{Si}$  data can be described as well by the prior interaction as by the post interaction form of DWBA. In the case of  $^{30}\text{Si}$  it was not possible to describe the correlation data with “symmetric” DWBA calculations which are able to reproduce the differential cross sections. Only coupled channels calculations which take multistep processes into account lead to a description of the angular correlation. A simulation of coupled channels by an asymmetric DWBA as proposed by Ascuitto *et al.* did not lead to a description in our cases. Even for the example discussed by these authors, namely, the scattering of  $^{16}\text{O}$  on  $^{40}\text{Ca}$ , remarkable differences remain in the predictions of the angular correlation between a full CC and a CC calculation simulating DWBA.

<sup>1</sup>F. H. Schmidt, R. E. Brown, J. B. Gerhart, and W. A. Kolasinski, Nucl. Phys. **52**, 353 (1964).

<sup>2</sup>W. W. Eidson, J. G. Cramer, D. E. Blatchley, and R. D. Bent, Nucl. Phys. **55**, 613 (1964).

<sup>3</sup>H. Wagner, A. Hofmann, and F. Vogler, Phys. Lett. **47B**, 497 (1973).

<sup>4</sup>R. N. Boyd, H. Clement, and G. D. Gunn, Nucl. Phys. **A283**, 434 (1977).

<sup>5</sup>S. Schneider, W. Eyrich, A. Hofmann, U. Scheib, and F. Vogler, Phys. Lett. **80B**, 180 (1979).

<sup>6</sup>W. Eyrich, A. Hofmann, U. Scheib, S. Schneider, F. Vogler, and H. Rebel, Phys. Lett. **63B**, 406 (1976); Nucl. Phys. **A287**, 119 (1977).

<sup>7</sup>U. Scheib, A. Hofmann, and F. Vogler, Phys. Rev. Lett. **34**, 1586 (1975).

<sup>8</sup>R. J. Ascuitto, J. F. Petersen, and E. A. Seglie, Phys. Rev. Lett. **41**, 1159 (1978).

<sup>9</sup>In connection with a special analysis these data have been already used in a prevailing theoretical work (Ref. 12). It was the intention of Ref. 12 to associate the formalism of coupled channels with a multishell description of the target nuclei.

<sup>10</sup>W. Eyrich, A. Hofmann, U. Scheib, S. Schneider, and F. Vogler, Nucl. Instrum. Methods **138**, 543 (1976).

<sup>11</sup>F. Rybicki, T. Tamura, and G. R. Satchler, Nucl. Phys. **A146**, 659 (1970).

<sup>12</sup>J. Stumm and A. Hofmann, Nucl. Phys. **A363**, 301 (1981).

<sup>13</sup>P. D. Kunz (unpublished).

<sup>14</sup>J. Raynal, ECIS77 (unpublished).

<sup>15</sup>U. Scheib, DWKS and CWKS (unpublished).

<sup>16</sup>M. Meyer, Diplomarbeit, Universität Erlangen-Nürnberg, 1980 (unpublished).

<sup>17</sup>S. Schneider, W. Eyrich, A. Hofmann, U. Scheib, and F. Vogler, Phys. Rev. C **20**, 71 (1979).

<sup>18</sup>H. Rebel, G. W. Schweimer, G. Schatz, J. Specht, R. Löhken,



- G. Hauser, D. Habs, and H. Klewe-Nebenius, Nucl. Phys. A182, 145 (1972).
- <sup>19</sup>D. Schwalm, E. K. Warburton, J. W. Olness, Nucl. Phys. A293, 425 (1977).
- <sup>20</sup>W. Eyrich, A. Hofmann, U. Scheib, S. Schneider, F. Vogler, and H. Rebel, Proceedings of the Europhysics Study Conference on the Structure of Lighter Nuclei, Hvar, Yugoslavia, 1978.
- <sup>21</sup>W. Eyrich, A. Hofmann, U. Scheib, S. Schneider, F. Vogler, and H. Rebel, J. Phys. Soc. Jpn. Suppl. 44, 640 (1978).
- <sup>22</sup>K. W. Schmid, L. Satpathy, and A. Faessler, Z. Phys. 267, 345 (1974).
- <sup>23</sup>B. H. Wildenthal, J. B. McGrory, and P. W. M. Glaudemans, Phys. Rev. Lett. 26, 96 (1971).
- <sup>24</sup>M. Berg, A. Hofmann, K. Thomas, H. Rebel, and G. W. Schweimer, Phys. Lett. 42B, 211 (1972).
- <sup>25</sup>M. P. Fewell, D. C. Kern, R. H. Spear, T. H. Zabel, A. M. Baxter, and S. Hinds, Phys. Rev. Lett. 43, 1463 (1979).
- <sup>26</sup>P. K. Glanz and George H. Rawitscher, Nucl. Phys. A217, 299 (1973).
- <sup>27</sup>H. Clement, G. Graw, W. Kretschmer, and W. Stach, J. Phys. Soc. Jpn. Suppl. 44, 570 (1978).
- <sup>28</sup>J. M. Lohr and W. Haeberli, Nucl. Phys. A232, 381 (1974).
- <sup>29</sup>K. Thomas, thesis, Universität Erlangen-Nürnberg 1972 (unpublished).
- <sup>30</sup>N. Austern, *Direct Nuclear Reaction Theories* (Wiley, New York, 1970).
- <sup>31</sup>K. E. Rehm, W. Henning, J. R. Erskine, and D. G. Kovar, Phys. Rev. Lett. 40, 1479 (1978).